Molecular Engineering Strategy for High Efficiency Fullerene-Free Organic Solar Cells Using Conjugated 1,8-Naphthalimide and Fluorenone Building Blocks

Author

Thu, Trang Do, Hong, Duc Pham, Manzhos, Sergei, Bell, John M, Sonar, Prashant

Griffith Research Online

https://research-repository.griffith.edu.au

Molecular Engineering Strategy for High Efficiency Fullerene-Free Organic Solar Cells Using Conjugated 1, 8-Naphthalimide and Fluorenone Building Blocks

Thu Trang Do,[a] Hong Duc Pham,[a] Sergei Manzhos,[b] John M. Bell,[a] and Prashant Sonar [a,c]*

[a]School of Chemistry, Physics and Mechanical Engineering, Queensland University of Technology (QUT), 2 George Street, Brisbane, QLD-4001, Australia.

[b]Department of Mechanical Engineering, Faculty of Engineering, National University of Singapore, Block EA #07-08, 9 Engineering Drive 1, Singapore 117576.

[c] Institute of Future Environment, GPO Box 2434, Brisbane QLD 4001

ABSTRACT:

We designed, synthesized and characterized a series of novel electron deficient small molecules non-fullerene acceptors based on 1,8-naphthalimide (NAI) and 9-fluorenone (FN) with different branched alkyl chains using various techniques. These molecules are based on an acceptor–donor–acceptor–donor–acceptor (A1–D–A2–D–A1) molecular design configuration with NAI as the end capping acceptor (A1), FN for electron-withdrawing central (A2) group and thiophene ring as a donor (D) unit. These materials are named as **NAI-FN-NAI (BO)** and **NAI-FN-NAI (HD)** where BO and HD represent butyloctyl and hexyldecyl alkyl

groups respectively. To further modify energy levels of materials, we converted the weak electron withdrawing ketonic group (C=O) attached to FN moiety of **NAI-FN-NAI (BO)** to a stronger electron withdrawing cyano group (C≡N) to obtain compound **NAI-FCN-NAI (BO)** by keeping the same alkyl chain. The optical, electrochemical and thermal properties of the new acceptors were studied. The materials exhibit higher to medium band gaps, lower lowest unoccupied molecular orbital (LUMO) energy levels and highly thermally stable properties. Organic solar cell devices employing conventional poly(3-hexylthiophene) (P3HT) a donor polymer and newly designed small molecules as the acceptor were investigated. Among all new materials, organic solar cell devices based on **NAI-FN-NAI (BO)** as an acceptor exhibit the highest performance with an open circuit voltage (V_{OC}) of 0.88V, a short-circuit current density (J_{SC}) of 9.1 mAcm^{-2}, a fill factor (FF) of 45%, and an overall power conversion efficiency (PCE) of 3.6%. This is the first report of 9-fluorenone based non-fullerene acceptor with P3HT donor in organic solar cell devices with such a promising performance.

INTRODUCTION

For the past two decades, extensive research efforts have been devoted to the improvement of solution-processed bulk heterojunction (BHJ) organic solar cells (OSCs) due to their advantages such as low cost, light weight and mechanical flexibility.[1,2] Concerning the choice of materials, till date the majority of the high performance OSC devices have been reported using a wide range of functional conjugated donor materials (either small molecules or polymers) with fullerene-based either [6,6]- phenyl-C61 butyric acid methyl ester (PC$_{61}$BM) or [6,6]- phenyl C71-butyric acid methyl ester (PC$_{71}$BM) molecules as the acceptor. PC$_{61}$BM and PC$_{71}$BM are the most commonly used acceptors in the OSC community due to their good electron mobility, superior electron affinity and an appropriate LUMO level. Currently, the best power conversion efficiency (PCE) of OSCs of about 10-11% has been achieved either by donor material development or through device engineering.[3-6] The electron acceptor plays as

crucial role, similarly to the electron donor material in obtaining high performance OSCs. However, compared with donor materials, the development of acceptor materials have lagged far behind and not many electron acceptors have been reported in the literature. Although fullerene derivatives have contributed substantially to the enhancement of OSC device performance, they have some limitations including the limited light absorption in the visible and NIR regions, high cost, difficulty to purify, and poor morphological stability.[7,8] To address these difficulties, various non-fullerene acceptors have been explored in the past few years and the efficiency of non-fullerene OSCs began to increase rapidly since the year 2010. Recently, the PCE value has been boosted to 7-9%,[9-12] and more recently, Zhao et. al. have achieved the world record PCE over 11%.[13] One of the most distinct advantages of using non-fullerene electron acceptor materials is the range of options available in selecting various aromatic building blocks, especially the n-type electron withdrawing conjugated moieties. Among various n-type building blocks, 1,8-naphthalimide (NAI) is a promising candidate for designing novel electron accepting materials, since NAI based small molecular acceptors usually possess a low-lying LUMO energy level, which can match the energy level of many wide band gap polymers.[14-16] In addition, alkyl side chains at the N-position of the NAI moiety will induce good material solubility which is important for homogeneous mixing with donor component for achieving appropriate nanomorphology. Recently, Kwon et al. reported efficient non-fullerene solar cells with a PCE value of 7.64% by utilising the NAI based (2*E*,2'*E*)-3,3'-(2,5-bis(hexyloxy)-1,4-phenylene)bis(2-(5-(4-(*N*-(2-ethylhexyl)-1,8-naphthalimide)yl)-thiophen-2-yl)acrylonitrile) (NIDCS-HO) as an electron acceptor with a donor polymer poly[(2,5-bis(2-hexyldecyloxy)phenylene)-*alt*-(5,6-difluoro-4,7-di(thiophen-2-yl)benzo[*c*]-[1,2,5]thiadiazole)] (PPDT2FBT). This result clearly indicates there is a great potential of NAI building block for designing and synthesizing new materials for OSCs application via molecular engineering strategy using promising cheap precursors.[17]

In order to design and synthesize a good acceptor, an appropriate electron accepting conjugated building blocks with high electron affinity need to be incorporated in the conjugated backbone which can modulate the appropriate LUMO value and can also retain the good electron mobility. One of the potential architectures for designing the new electron acceptor is building blocks with acceptor-donor-acceptor-donor-acceptor structure (A1-D-A2-D-A1)[18] (where A1 and A2 have different electron affinities). With this configuration, electronic energy levels and band gaps can be easily tuned by modifying the core and terminal electron acceptor units.[19] Taking the A1-D-A2-D-A1 molecular design strategy into account, we synthesized a series of novel electron acceptors based on NAI as the electron-withdrawing terminal group attached to a donor thiophene unit in combination with 9-fluorenone and dicyanofluorene as the weak and strong electron withdrawing central building blocks (see Figure 1). The 9-fluorenone incorporated newly designed compounds with two different branched butyl octyl (BO) and hexyl decyl (HD) alkyl chains have been named as 6,6'-((9-oxo-9*H*-fluorene-2,7-diyl)bis(thiophene-5,2-diyl))bis(2-(2-butyloctyl)-1*H*-benzo[*de*]isoquinoline-1,3(2*H*)-dione) (**NAI-FN-NAI (BO)**) and 6,6'-((9-oxo-9*H*-fluorene-2,7-diyl)bis(thiophene-5,2-diyl))bis(2-(2-hexyldecyl)-1*H*-benzo[*de*]isoquinoline-1,3(2*H*)-dione) (**NAI-FN-NAI (HD)**), respectively. The 9-fluorenone central block has been used due to its higher chemical stability,[20,21] energy level tunability,[22,23] and simple preparation[22,24]. The thiophene spacer was used with NAI because of its relatively strong interchain interaction and high charge carrier mobility well proven in BHJ OSCs.[25,26]
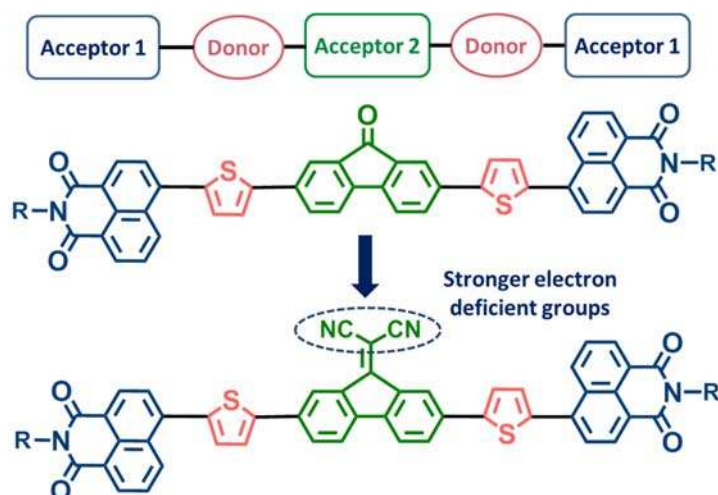
**Fig. 1**: Molecular Engineering approach to design novel electron acceptors

In order to further modify energy levels of the materials, we converted the ketonic group (C=O) substituted on 9-fluorenone moiety of **NAI-FN-NAI (BO)** to the stronger electron withdrawing cyano groups via cyanation, and this successfully yielded a new compound 2-(2,7-bis(5-(2-(2-butyloctyl)-1,3-dioxo-2,3-dihydro-1*H*-benzo[*de*]isoquinolin-6-yl)thiophen-2-yl)-9*H*-fluoren-9-ylidene)malononitrile (**NAI-FCN-NAI (BO)**). In this work, we discuss the synthesis of new non-fullerene acceptors along with their complete thermal, optical, electrochemical properties using different characterization techniques. Finally, we have evaluated the newly synthesized non-fullerene acceptors with P3HT donor blends in OSC BHJ devices and their photovoltaic properties are discussed in detail. With a P3HT donor, Holliday et. al. have reported the highest PCE of 6.3 % with a non-fullerene acceptor,[27] whereas our new non-fullerene acceptor exhibits a still impressive PCE of 3.6 %. The measured PCE is promising because there are still relatively unstudied materials, which have not yet undergone extensive optimization. The nanomorphology of the blend is also studied in detail using the atomic force microscopy (AFM) technique.

RESULTS AND DISCUSSION

New non-fullerene Acceptor Molecular Design and Synthesis:

Scheme 1 depicts the synthetic routes to a series of new acceptor materials based on three conjugated segments including NAI and FN with two different alkyl chains. Two different alkyl groups were chosen in order to evaluate the effect of alkyl chain length on the solubility, miscibility with donor polymer in blends, and tunability of their crystallinity. In order to induce the solution processability to the NAI core, first alkyl alcohols were converted to their respective alkyl bromides (**1**) and then reacted with potassium phthalimide to give alkylphthalimide derivatives (**2**). These compounds were reduced by hydrazine monohydrate to form respective alkyl amines (**3**). The alkylnaphthalimide group (**4**) was prepared by reacting 4-bromo-1,8-naphthalic anhydride with either 2-butyl-octylamine or 2-hexyl-decylamine in gram-scale quantities. Then, the alkylated naphthalimide was subjected to Stille coupling reaction with commercially available tributyltin thiophene in the presence of a palladium catalyst to produce alkyl substituted thiophene naphthalimide (**5**). This compound was further converted to its monobromo derivative (**6**) using *N*-bromosuccinamide (NBS) as the starting precursor. Another starting precursor, 2,7-bis(4,4,5,5-tetramethyl-1,3,2-dioxaborolan-2-yl)-9*H*-fluoren-9-one, was synthesized using bispinacolatodiboron, potassium acetate and $PdCl_2$ (dppf) catalyst from 2, 7-dibromo fluorenone with a good yield. Afterward, butyl octyl and hexyl decyl branched alkyl substituted monobromo-thiophene naphthalimide were reacted with 2,7-bis(4,4,5,5-tetramethyl-1,3,2-dioxaborolan-2-yl)-9*H*-fluoren-9-one via Suzuki coupling and the target compounds **NAI-FN-NAI (BO)** and **NAI-FN-NAI (HD)** were obtained. Another **NAI-FCN-NAI (BO)** target compound with strong electron withdrawing dicyano functionality on fluorine was prepared from fluorenone substituted **NAI-FN-NAI (BO)** compound using malononitrile in DCM in the presence of titanium tetrachloride and pyridine. All compounds show good solubility in common organic solvents such as chloroform, dichloromethane,

toluene, tetrahydrofuran, etc. and which allowed fabricating solution-processed small molecule OSC devices. The purity of all the synthesized precursors as well as final semiconductors were confirmed by proton and carbon NMR spectroscopy.
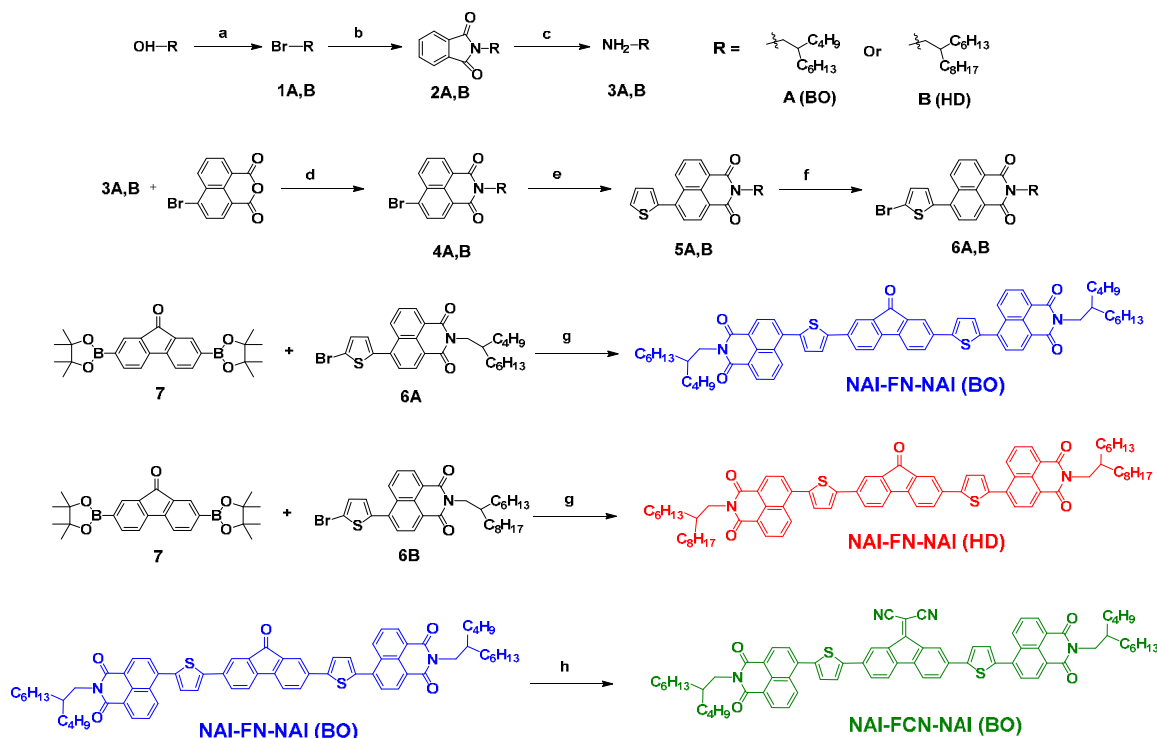
Scheme 1. Synthetic route of building blocks. Reagent and conditions: (a) Triphenylphosphine, Br$_2$, DCM, 0 °C ~ room temp., overnight, 95%; (b) Potassium phthalimide, DMF, 90 °C 24h, 90%; (c) NH$_2$NH$_2$·H$_2$O, MeOH, refluxed, 8h, 100%; (d) Anhydrous DMF, 110 °C, overnight, 60%; (e) 2-Tributylstannylthiophene, Pd(dppf)Cl$_2$, Toluene, refluxed, 10h, 65%; (f) NBS, DMF, room temp., overnight, 80%; (g) 2M K$_2$CO$_3$, toluene, Pd(PPh$_3$)$_4$, 110 °C, 48 h, 65%; (h) Malononitrile, CH$_2$Cl$_2$, TiCl$_4$, pyridine, 0 °C ~ room temp., 10h, 76%.

<u>Thermal Properties</u>:

The thermal properties of all newly synthesized acceptor materials were investigated using thermogravimetric analysis (TGA) and differential scanning calorimetry (DSC). All three acceptor materials showed an excellent thermal stability and the decomposition temperatures (T_d) with 5% weight loss were observed above 420 °C (Fig. 2). Such a high thermal stability is arising from the fused aromatic fluorenone core attached to thiophene and NAI end capping group. During DSC heating and cooling scans, **NAI-FN-NAI (BO)** and **NAI-FN-NAI (HD)** showed crystallization peaks at 193 °C and 200 °C whereas melting peaks were observed at 214 °C and 216 °C, respectively (Fig. 3). This result clearly demonstrated that the slight change of alkyl chain length did not alter thermal properties. **NAI-FCN-NAI (BO)** exhibited higher melting and crystallization points at 257 °C and 224 °C, respectively, indicating the more rigid structure of **NAI-FCN-NAI (BO)** than **NAI-FN-NAI (BO)** and **NAI-FN-NAI (HD)** compounds. The central dicyanofluorene conjugated moiety is responsible for enhancing the high thermal stability **NAI-FCN-NAI (BO)**. The high thermal stability of these novel compounds might be very helpful in preventing degradation of the active layer of blends with donor polymers in OSCs devices upon annealing.
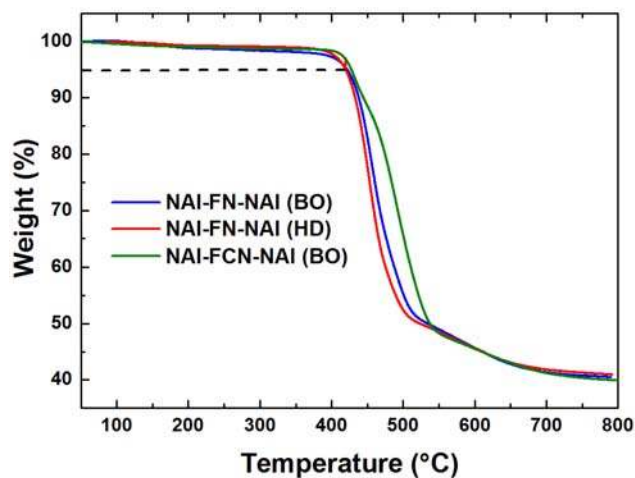
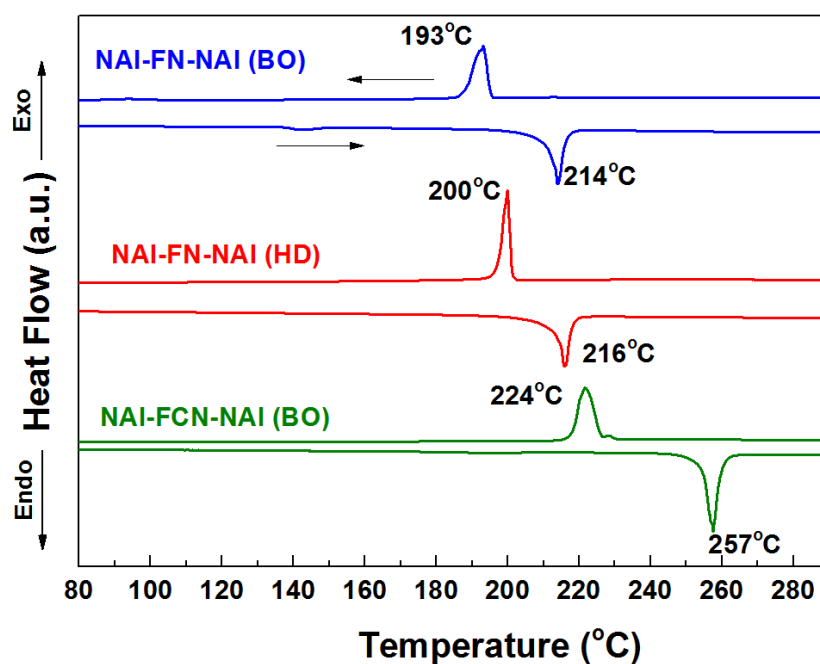**Fig. 2**: TGA thermograms of **NAI-FN-NAI (BO), NAI-FN-NAI (HD)** and **NAI-FCN-NAI (BO)**.

Fig. 3: Differential Scanning Calorimetric (DSC) analysis of **NAI-FN-NAI (BO), NAI-FN-NAI (HD)** and **NAI-FCN-NAI (BO)**.

<u>Optical Properties:</u>

The absorption spectra of the compounds in a chloroform solution and in thin film are shown in Fig. 4. **NAI-FN-NAI (BO)** and **NAI-FN-NAI (HD)** exhibit very similar absorption spectra with the maximum absorption peaks around 425 nm, whereas **NAI-FCN-NAI (BO)** shows a similar maximum absorption peak around 425 nm with an additional peak at 585 nm. The similar absorption of **NAI-FN-NAI (BO)** and **NAI-FN-NAI (HD)** compounds are due to an identical conjugated backbone and the only difference in their structure being the nature of alkyl chain which doesn't play a role in optical tuning. The extra peak of **NAI-FCN-NAI (BO)** compound in the absorption spectrum is achieved by converting the ketonic group to the cyano group. In thin film, the maximum absorption peaks in the longer wavelength region of **NAI-FN-NAI (BO)**, **NAI-FN-NAI (HD)** and **NAI-FCN-NAI (BO)** were 426 nm, 425 nm and 427-625 nm, respectively. Comparing with the absorption spectra in solution, these peaks are red shifted by about 14-39 nm due to the enhancement of intermolecular interaction in the solid state. The absorption band-edge of the cast films for **NAI-FN-NAI (BO)**, **NAI-FN-NAI (HD)** and **NAI-FCN-NAI (BO)** are 582, 585 and 773 nm respectively, corresponding to the optical bandgaps (E_g^{opt}) of 2.13, 2.12 and 1.61 eV. The lowest band gap of **NAI-FCN-NAI (BO)** clearly shows that by simply tuning from a weak electron withdrawing ketonic group to a strong electron withdrawing cyano group, the optical band gap can be reduced dramatically. The higher band gap nature of **NAI-FN-NAI (BO)** and **NAI-FN-NAI (HD)** compounds may be arising from the lower interaction between NAI end capping group and central fluoreneone core attached to thiophene. Absorption at shorter wavelength is due to the lower conjugation length arising from the twisted conjugated backbones. In spite of higher optical band gap, they can be suitable electron transporting materials due to the strong withdrawing moieties incorporated in their backbone and the materials appropriate electron mobility and energy levels.
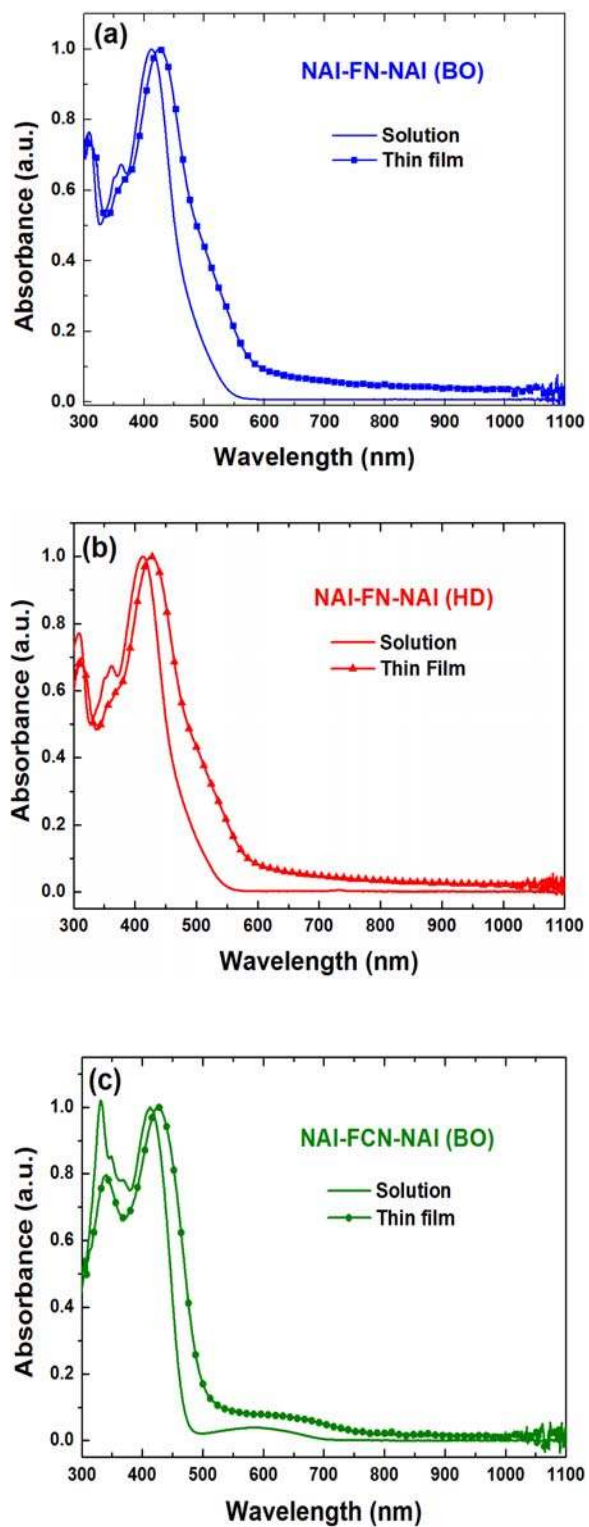
Fig. 4: UV-Vis absorption spectra of (a) **NAI-FN-NAI (BO)**, (b) **NAI-FN-NAI (HD)**

and (c) **NAI-FCN-NAI (BO)** in chloroform solutions and as thin films.

Electrochemical Properties:

The electrochemical properties of all three compounds were investigated by cyclic voltammetry (CV) with a glassy carbon working electrode using 0.1 M tetra(n-butyl)ammonium hexafluorophosphate (n-Bu$_4$NPF$_6$) in DCM solution as an electrolyte at a potential scan rate of 100 mV/s. The reference electrode (Ag/Ag$^+$) was calibrated by the ferrocene/ferrocenium (Fc/Fc$^+$) redox couple (4.8 eV below the vacuum level). As shown in Fig. 5, compounds **NAI-FN-NAI (BO)**, **NAI-FN-NAI (HD)** and **NAI-FCN-NAI (BO)** exhibited quasi-reversible reduction and oxidation waves. The oxidation and reduction onset values were calculated by taking intersection of baseline to the rising current point from CV data. The HOMO and LUMO values for all materials were calculated using oxidation and reduction onset values using the relation HOMO = -E_{HOMO} = e ($E_{onset (ox)}$ + 4.8) eV and E_{LUMO} = e ($E_{onset(red)}$ + 4.8) eV. The HOMO values of compounds **NAI-FN-NAI (BO)**, **NAI-FN-NAI (HD)** and **NAI-FCN-NAI (BO)** were -6.07, -6.06 and -6.14 eV, respectively, whereas the LUMO values were -3.96, -3.98 and -4.21 eV, respectively. The extremely lower HOMO values of all materials are due to the strong electron withdrawing nature of newly synthesized electron acceptors. The obtained LUMO values are appropriate and significantly lower for better charge separation and electron transport. Furthermore, it is clear that the change of alkyl chain did not affect the HOMO and LUMO energies. However, compared to **NAI-FN-NAI (BO)**, **NAI-FCN-NAI (BO)** demonstrated lower-lying HOMO and LUMO energies; which is possibly due to the stronger electron withdrawing properties of cyano substituted compound than that of ketonic group substituted materials.[28-30] The optical (absorbance maxima, optical band gaps) and electrochemical (HOMO-LUMO levels, electrochemical band gaps) properties of these newly synthesized materials are shown in Table 1. The optical and electrochemical band gaps of **NAI-FN-NAI (BO)**, **NAI-FN-NAI (HD)** and **NAI-FCN-NAI (BO)** materials are matching very well. The energy levels of these new acceptor materials were compared with

donor polymer P3HT HOMO-LUMO values and work functions of metal anode/cathode electrodes (See Fig. 6).
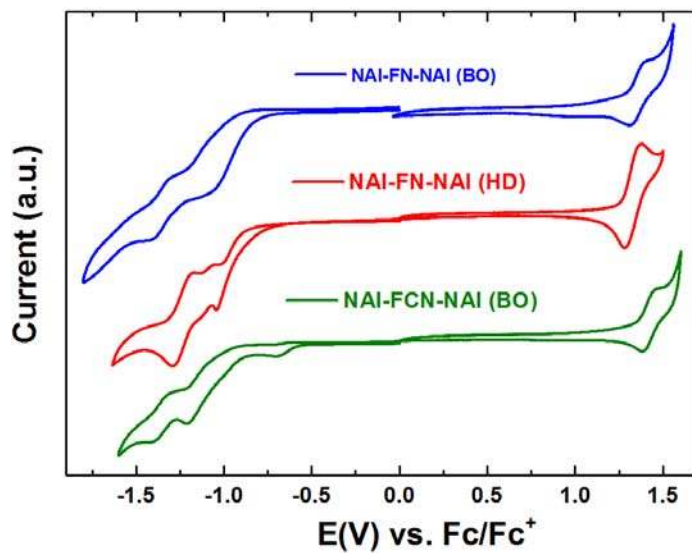

Fig. 5: Cyclic voltammograms of **NAI-FN-NAI (BO), NAI-FN-NAI (HD)** and **NAI-FCN-NAI (BO)**.
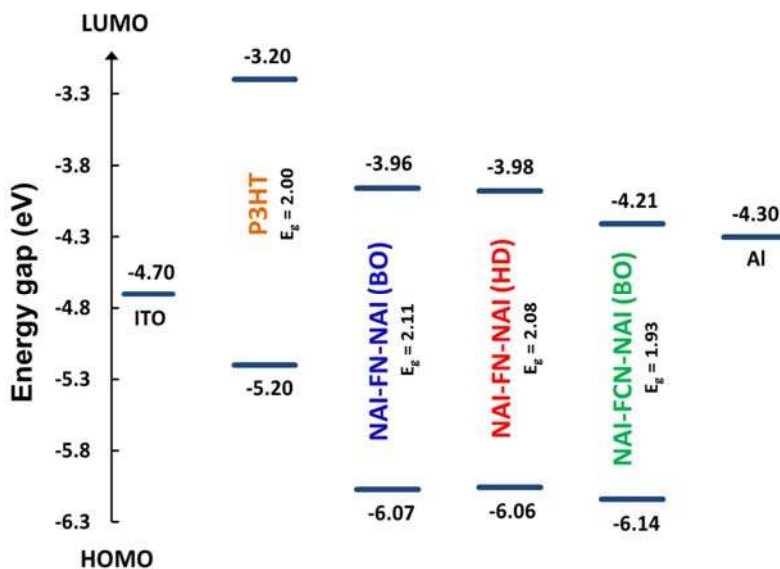

Fig. 6: Schematic energy level diagram of **NAI-FN-NAI (BO), NAI-FN-NAI (HD)** and **NAI-FCN-NAI (BO)** based device.

Table 1. Optical and electrochemical data for the molecules **NAI-FN-NAI (BO), NAI-FN-NAI (HD), NAI-FCN-NAI (BO)**

Compound	λ_{max} (nm)		E_g^{opt} (eV)	E_g^{cv}[a] (eV)	HOMO (eV)	LUMO (eV)
	Solution	Film				
NAI-FN-NAI (BO)	411	426	2.13	2.11	-6.07	-3.96
NAI-FN-NAI (HD)	411	425	2.12	2.08	-6.06	-3.98
NAI-FCN-NAI (BO)	412, 586	427, 625	1.64	1.93	-6.14	-4.21

[a] Electrochemical bandgap = │HOMO - LUMO│

Theoretical calculations:

In order to further understand the properties of these newly synthesized materials, calculations based on density functional theory[31,32] at the B3LYP[33] (frontier orbital energies) levels of theory using the basis set 6-31g+(d,p) were performed. A polarized continuum model of the chloroform solvent was used.[34] The calculations were performed in Gaussian 09.[35] Since the alkyl chain does not participate in the conjugation backbone so herein we have selected two compounds having common buty octyl chain and central cores with different electron affinities (fluoreneone vs dicyanofluorene) As shown in Fig. 7, the HOMO and LUMO of **NAI-FN-NAI (BO)** are delocalized along the entire backbone, whereas the LUMO of **NAI-FCN-NAI (BO)** is much more localized around the central functionalized cyano substituted fluorene and its HOMO is much better delocalized. The computational results show that the HOMO/LUMO energy levels of **NAI-FN-NAI (BO)** and **NAI-FCN-NAI (BO)** were -5.82/-3.05 eV and -5.87/-3.65 eV, respectively. The theoretical calculated HOMO-LUMO values of these new acceptors are overestimated compared to the experimentally derived but the computed HOMO-LUMO value validate the effect of different donor-acceptor building blocks observed experimentally. The overestimated of the computed levels can be attributed to the limits of the model (basis

size and underlying DFT approximations). The dihedral angles between thiophene ring and two central building blocks FN and FCN were 25.4° and 26.5°, respectively.
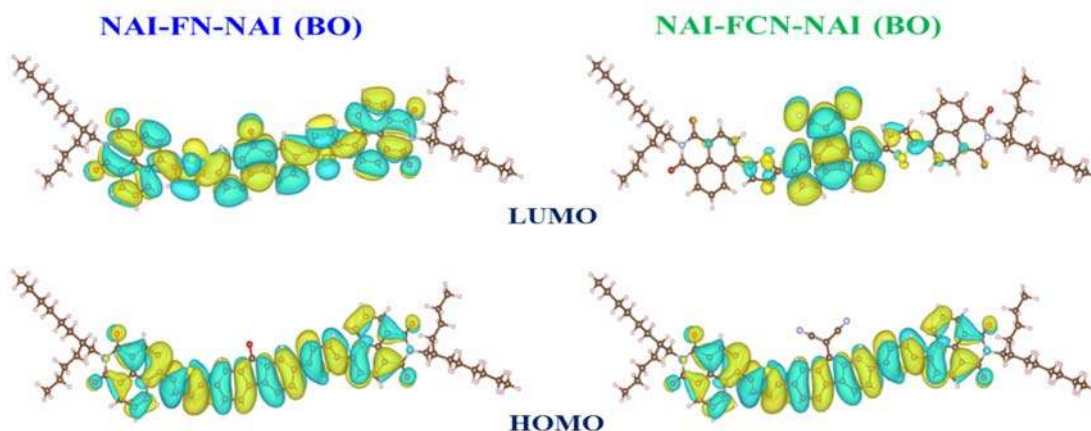

Fig. 7: Comparison of calculated energy levels HOMO and LUMO orbital surfaces of **NAI-FN-NAI (BO)** or **NAI-FCN-NAI (BO)** using the DFT method.

Photovoltaic Properties:

Bulk heterojunction (BHJ) solar cells were fabricated using P3HT as the electron donor material and **NAI-FN-NAI (BO)** / **NAI-FCN-NAI (BO)** / **NAI-FN-NAI (HD)** as the electron acceptor material using standard OSC device fabrication conditions. Schematic diagram of the solar cells with the conventional device architecture [ITO/PEDOT:PSS/active layer/LiF/Al] is shown in Fig. 8a. The ITO coated glass acts as anode whereas PEDOT:PSS work function modifying layer. The LiF and Al are electron blocking layer and cathode electrode respectively. In other words, PEDOT:PSS and LiF layers acts as hole and electron collecting layers, since after exciton dissociation in OSCs, the separate individual charges need to be collected effectively at respective electrodes. The active layer is a blend of conventional P3HT donor and the newly developed **NAI-FN-NAI (BO)** / **NAI-FCN-NAI (BO)** / **NAI-FN-NAI (HD)** electron acceptors. Upon complete fabrication OSC devices, the devices were characterized using standard electrical current density (J) – voltage (V) characteristics. The current density–

voltage characteristics of the devices under simulated solar illumination (AM 1.5G, 1000 W m^{-2}) are shown in Fig. 8b and the photovoltaic performance of these devices is summarized in Table 2. The **P3HT:NAI-FCN-NAI (BO)** (1:1) based OSC devices exhibits lowest performance among all devices with an open-circuit voltage (V$_{OC}$) value of 0.56 V, a fill factor (FF) of 36%, a short-circuit current density (J$_{SC}$) value of 3.0 mA.cm^{-2} and a power conversion efficiency (PCE) value of 0.6%. The lowest performance might be attributed with the deep LUMO value of **NAI-FCN-NAI (BO)** compound, which gives lower open circuit voltage. Other reasons for lower performance could be due to slightly higher crystalline nature of **NAI-FCN-NAI (BO)** arising from strong $\pi-\pi$ stacking and intramoleculer donor-acceptor interactions. The molecular structure is more rigid and also alkyl chain substituted on nitrogen is smalleras per molecular rigidity concern. The **P3HT:NAI-FN-NAI (HD)** (1:1) based OSC devices exhibits four times higher performance devices than the **P3HT:NAI-FCN-NAI (BO)** devices with an open-circuit voltage (V$_{OC}$) value of 0.86 V, a fill factor (FF) of 41%, a short-circuit current density (J$_{SC}$) value of 7.2 mA.cm^{-2} and a power conversion efficiency (PCE) value of 2.5%. The 1.5 times higher V$_{OC}$ of **P3HT:NAI-FN-NAI (HD)** (1:1) devices compared to **P3HT:NAI-FCN-NAI (BO)** (1:1) devices are a clear indication of the effect of LUMO energy level variations. The V$_{OC}$ of OSC device is controlled by the difference between HOMO of donor and LUMO of acceptor. The short circuit current of **P3HT:NAI-FN-NAI (HD)** devices are almost doubled than **P3HT:NAI-FCN-NAI (BO)** (1:1) devices which are attributed to the better donor-acceptor blend compability and appropriate energy levels. Among all OSC devices, the **P3HT:NAI-FN-NAI (BO)** device showed the highest performance using newly developed acceptor with an open-circuit voltage (V$_{OC}$) value of 0.88 V, a fill factor (FF) of 45%, a short-circuit current density (J$_{SC}$) value of 9.1 mA.cm^{-2} and a power conversion efficiency (PCE) value of 3.6%. Since the LUMO of **NAI-FN-NAI (BO) and NAI-FN-NAI (HD)** acceptors are comaprable so there is a similar V$_{OC}$ values (0.88 *vs* 0.86). The **NAI-FN-**

NAI (BO) acceptor showed a better device performance among all is due to the higher J_{SC} (9.1 mA.cm^{-2}) and FF (45). This effect is related to the enhanced nano-scale morphology of the active layer confirmed by the atomic force microscope (AFM). The height and phase AFM images of **P3HT:NAI-FN-NAI (BO)** blended film are shown in Fig. 9 (a) and (b) and, they clearly exhibits better phase separated morphology with nano-scale domains compared to other blended devices.

Table 2. Solar cell performance of non-fullerene acceptors **NAI-FN-NAI (BO)**, **NAI-FN-NAI (HD)** and **NAI-FCN-NAI (BO)** (Average value of 6 devices for each acceptor means total 18 devices for three acceptors)

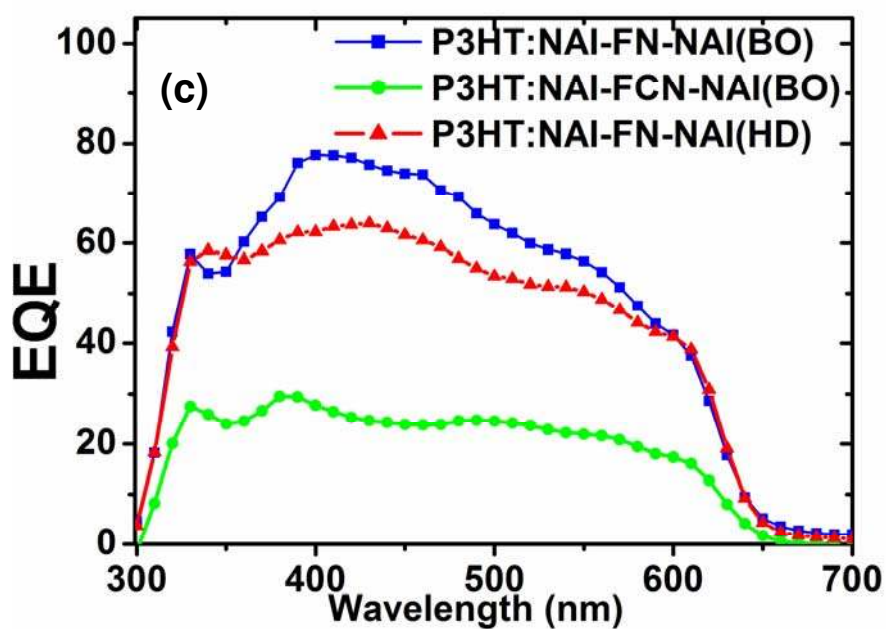| Active Layer Blend Ratio	J_{SC} (mA/cm^2)	V_{OC} (V)	FF (%)	PCE (%)
P3HT:NAI-FN-NAI (BO) (1:1)	9.1 ± 0.20	0.88 ± 0.02	45 ± 2	3.6 ± 0.20
P3HT:NAI-FN-NAI (HD) (1:1)	7.2 ± 0.35	0.86 ± 0.02	41 ± 2	2.5 ± 0.30
P3HT:NAI-FCN-NAI (BO) (1:1)	3.0 ± 0.25	0.56 ± 0.02	36 ± 3	0.6 ± 0.2
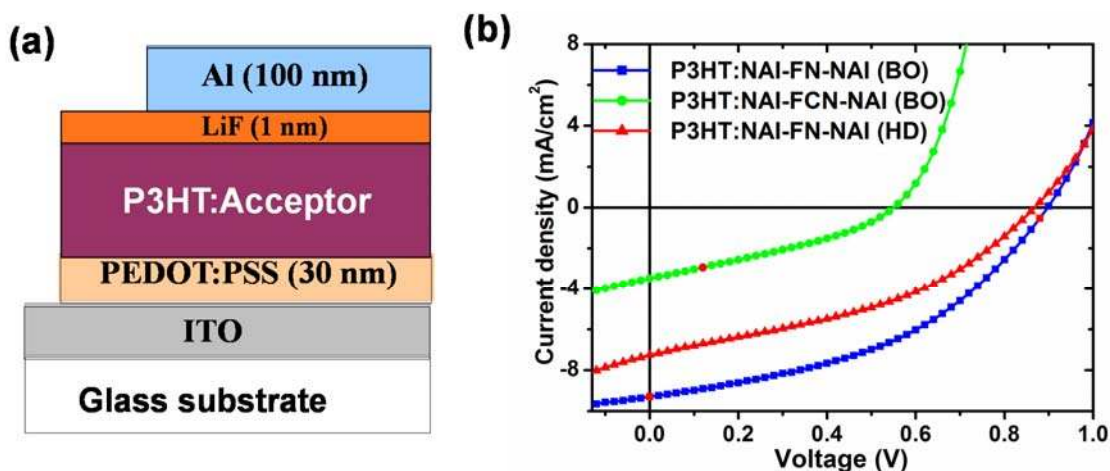
Fig. 8: (a) Schematic diagram of conventional device geometry; (b) J-V curves of the BHJ solar cells and (c) external quantum efficiency (EQE) curves of **NAI-FN-NAI (BO)**, **NAI-FCN-NAI (BO)** and **NAI-FN-NAI (HD)** non-fullerene acceptor based OSCs devices.
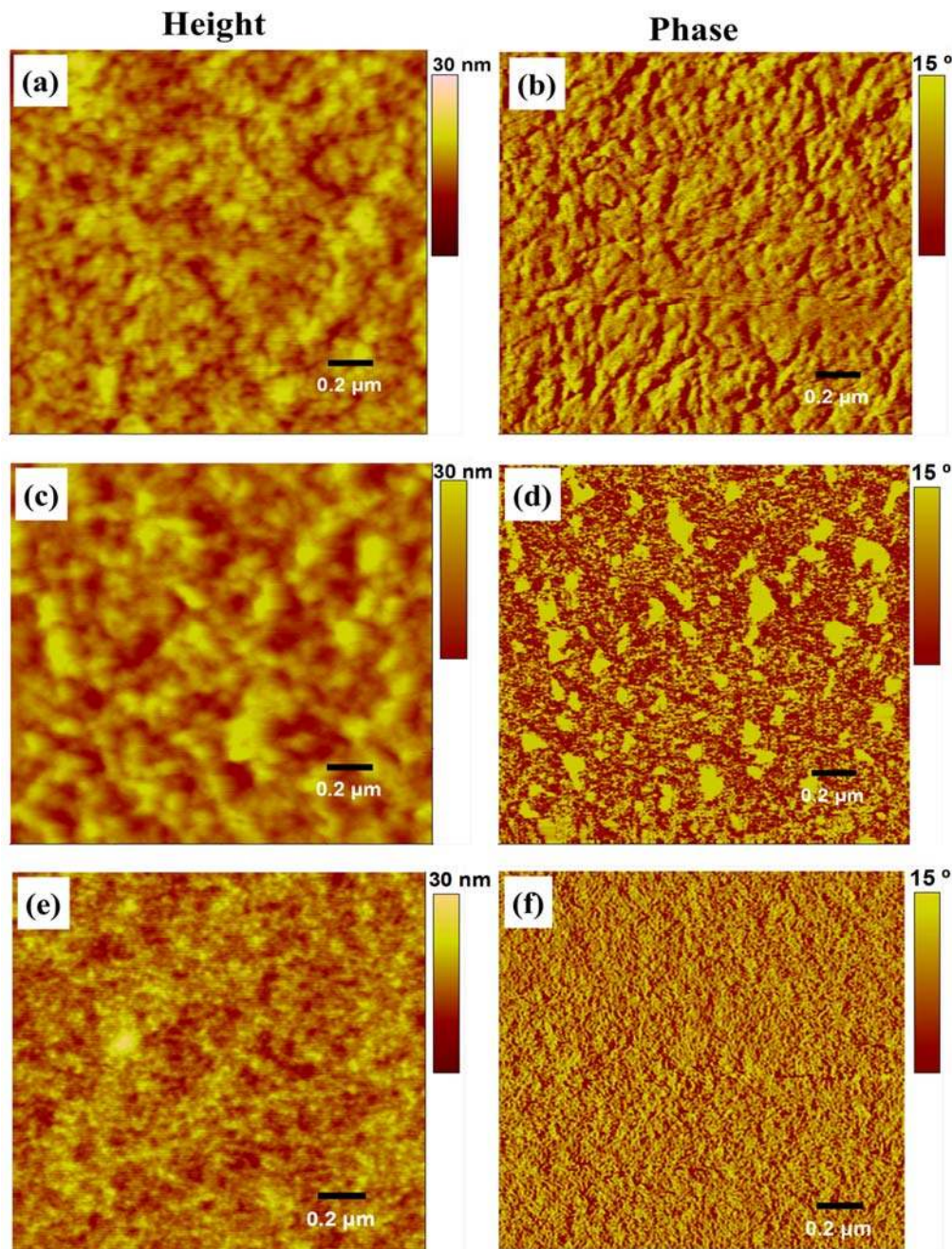
Fig. 9: AFM height images of (a) **P3HT:NAI-FN-NAI (BO)**, (c) **P3HT:NAI-FN-NAI (HD)** and (e) **P3HT:NAI-FCN-NAI (BO)** and AFM phase images of (b) **P3HT:NAI-FN-NAI (BO)**, (d) **P3HT:NAI-FN-NAI (HD)** and (f) **P3HT:NAI-FCN-NAI (BO)**

CONCLUSIONS

New electron deficient small molecules with acceptor–donor–acceptor–donor–acceptor architecture based on thiophene donor, naphthalimide and fluorenone or fluorenylidene-malononitrile acceptor moieties with butyloctyl (BO) and hexyldecyl (HD) alkyl groups, **NAI-FN-NAI (BO)**, **NAI-FN-NAI (HD)** and **NAI-FCN-NAI (BO)**, were synthesized and characterized. All three compounds have shown an excellent thermal stability and the decomposition temperatures with 5% weight loss were observed above 420 °C. **NAI-FN-NAI (BO)**, **NAI-FN-NAI (HD)** had the similar absorption band in the range of 300-600nm, whereas **NAI-FCN-NAI (BO)** showed two absorption bands of 300-500 nm and 500-750 nm. The HOMO/LUMO values of compounds **NAI-FN-NAI (BO)**, **NAI-FN-NAI (HD)** and **NAI-FCN-NAI (BO)** were -6.07/-3.69, -6.06/-3.98 and -6.14/-4.21 eV, respectively. In comparison to other compounds, **NAI-FCN-NAI (BO)** demonstrated lower-lying HOMO and LUMO energies due to the stronger electron withdrawing properties of cyano substituted compound than that of ketonic group substituted materials. The OSCs based on **P3HT:NAI-FN-NAI (BO)** (1:1, w/w) with thermal annealing at 140 °C for 10 min exhibited the highest PCE of 3.6% with a high J_{SC} of 9.1 mA.cm^{-2} and V_{OC} of 0.88 V which is attributed to the enhanced nano-scale morphology of the active layer.

EXPERIMENTAL SECTION

Materials and Instruments

All staring materials were purchased commercially as analytical reagents and used directly without any further purification. Compound 2,7-bis-(4,4,5,5-tetramethyl-[1,3,2]dioxaborolan-2-yl)-fluoren-9-one (**4**) was prepared according to the literature.[22] Synthesized compounds were characterized by ^{1}H-NMR and ^{13}C-NMR spectrum, which were obtained with a Varian-400 spectrometer. The elemental analysis of the

synthesized compounds was carried out on an Elementar Vario macro/micro elemental analyser. Thermal analysis was performed using a Pegasus Q500TGA thermogravimetric analyzer under nitrogen atmosphere at a heating rate of 10 °C/min. Differential scanning calorimetry (DSC) was conducted under nitrogen using a Chimaera instrument Q100 DSC. The sample was heated at 10 °C/min from 30 °C to 300 °C. Absorption spectra were recorded on Carry50 UV-Vis Spectrophotometer.

Device Fabrication

Bulk-heterojunction (BHJ) solar cells were fabricated by spin coating of 30-nm-thick layers of poly(3,4-ethylenedioxythiophene):poly(styrenesulfonate) (PEDOT:PSS; Baytron AI 4083 from HC Starck) on ITO (Indium Tin Oxide) patterned glass substrates which were washed by acetone, and 2-propanol in an ultrasonication bath and UV/ozone-treated. The PEDOT:PSS films were baked at 140 °C for 10 min in air. An active layer of the device consisting of a blend of P3HT and small molecule acceptor (**NAI-FN-NAI (BO)** / **NAI-FN-NAI (HD)** / **NAI-FCN-NAI (BO)**)) with a ratio of 1:1 was then spin coated from chlorobenzene solvent with a thickness of ~ 95 nm. The films were transferred to a metal evaporation chamber and top electrode consist of LiF (1 nm) and aluminum (100 nm) were deposited through a shadow mask (device area was 0.1 cm^2) at approximately 1 x10^{-6} torr. Film thickness was determined by Veeco Dektak 150+Surface Profiler. The current density-voltage measurements of the devices were carried out using a 1 kW Oriel solar simulator with an AM 1.5G filter as the light source in conjunction with a Keithley 2400 source measurement unit. Solar measurements were carried out under 1000 W/m^2 AM 1.5G illumination conditions. For accurate measurement, the light intensity was calibrated using a reference silicon solar cell (PV measurements Inc.) certified by the National Renewable Energy Laboratory. Device fabrication and characterizations were performed in an ambient environment without any encapsulation.

Morphology Characterisation

The AFM samples were prepared by spin coating the blend solution on PEDOT:PSS layer. Tapping-mode AFM (NanoScope III, Dimension, Digital Instrument Inc.) was carried out with commercially available tapping mode tips.

Synthesis

Synthesis of 5-(bromomethyl)undecane (1A)

Triphenylphosphine (26.23 g, 0.1 mol) was dissolved in DCM (200 mL) under argon for 15 minutes. Then the reaction mixture was cooled to 0 $^{\circ}$C and followed by the addition of bromine (7.2 mL, 0.14 mol). After 2-butyloctan-1-ol (18.63 g, 0.1 mol) was added dropwise via an additional funnel over 30 minutes, the reaction solution was stirred at room temperature for overnight under argon. The organic solvent was removed under reduced pressure, and the residue was extracted with excess amount of hexane. The hexane was evaporated and the resulting crude yellow oil was purified by silica gel column eluting with hexane. The title compound was isolated as colourless oil (23.75 g, 95.3%). ^{1}H NMR (400 MHz, CDCl$_3$, ppm): δ 3.45-3.44 (d, J = 4.8 Hz, 2H), 1.61-1.56 (m, 1H), 1.28 (m, 16H), 0.92-0.87 (m, 6H).

Synthesis of 7-(bromomethyl)pentadecane (1B)

The synthetic procedure is similar to that described for **1A**. Yield: 29.0 g, 95%. ^{1}H NMR (400 MHz, CDCl$_3$, ppm): δ 3.45-3.44 (d, J = 4.8 Hz, 2H), 1.59 (m, 1H), 1.27 (m, 24H), 0.90-0.86 (m, 6H).

Synthesis of 2-(2-butyl-octyl)isoindole-1,3-dione (2A)

To a mixture of 1-bromo-2-butyloctane (7.48 g, 30.0 mmol) and potassium phthalimide (5.93 g, 32 mmol), 45 mL of DMF was added and stirred at 90 $^{\circ}$C for 10 hours. Then the reaction mixture was cooled to room temperature and extracted with DCM and water. The combined organic layer was washed with 0.2 N KOH aqueous (100 mL), water (100 mL) and saturated NH$_4$Cl aqueous (100 mL). The organic layer was dried over anhydrous Na$_2$SO$_4$ and

concentrated by evaporation. The crude product was purified by silica gel chromatography using a mixture of hexane and chloroform as eluent to obtain product as colourless oil (8.52 g, 90%). ^{1}H NMR (400 MHz, CDCl3, ppm): δ 7.85-7.83 (m, 2H), 7.71-7.69 (m, 2H), 3.57-3.55 (d, J = 7.2 Hz, 2H), 1.87 (m, 1H), 1.26 (m, 16H), 0.88-0.83 (m, 6H).

Synthesis of 2-(2-hexyl-decyl)isoindole-1,3-dione (2B)

The synthetic procedure is similar to that described for **2A**. Yield: 9.81 g, 90%. ^{1}H NMR (400 MHz, CDCl3, ppm): δ 7.84-7.82 (m, 2H), 7.70-7.68 (m, 2H), 3.56-3.54 (d, J = 7.2 Hz, 2H), 1.86 (m, 1H), 1.22 (m, 24H), 0.86-0.82 (m, 6H).

Synthesis of 2-butyl-octylamine (3A)

To a solution of 2-(2-butyl-octyl)isoindole-1,3-dione (6.31 g, 20.0 mmol) in MeOH (90 mL), hydrazine monohydride (3.0 g, 60.0 mmol) was added and refluxed overnight. After cooling to room temperature, the mixture was evaporated under vacuum. The residue was dissolved in DCM and washed with 10 wt% KOH aq. (100 mL x2) and saturated NaCl aq. (100 mL x2). The organic layer was dried with anhydrous Na2SO4 and concentrated by vacuum evaporation to obtain colourless oil (3.89 g). This compound was used for subsequent reaction without further purification. ^{1}H NMR (400 MHz, CDCl3, ppm): δ 2.56-2.55 (d, J = 2.8 Hz, 2H), 1.22 (m, 19H), 0.87-0.82 (m, 6H).

Synthesis of 2-hexyl-decylamine (3B)

The synthetic procedure is similar to that described for **3A**. Yield: 5.79 g. ^{1}H NMR (400 MHz, CDCl3, ppm): δ 2.57 (d, J = 4.0 Hz, 2H), 1.24 (m, 27H), 0.87-0.84 (m, 6H).

Synthesis of 6-bromo-2-(2-butyloctyl)-1H-benzo[de]isoquinoline-1,3(2H)-dione (4A)

To a solution of 4-bromo-1,8-naphthalic anhydride (4.16 g, 15.0 mmol) in DMF (60 mL), 2-butyl-octylamine (3.34 g, 18.0 mmol) was added dropwise. Then the reaction mixture was

heated to 110 °C and stirred under nitrogen overnight. Then the reaction mixture was cooled to room temperature and concentrated using a rotary evaporator. The product was precipitated into 1N HCl, filtered off, and washed with 1N HCl. The crude product was purified by silica gel column chromatography using ethyl acetate and hexane mixture (vol. ratio 1:9) as an eluent. After recystallization from the eluent mixture of solvents, yellow crystals were obtained (4.0 g, 60%). ^{1}H NMR (400 MHz, CDCl$_3$, ppm): δ 8.66-8.64 (d, J = 7.2 Hz, 1H), 8.57-8.55 (d, J = 8.8 Hz, 1H), 8.41-8.40 (d, J = 8.0 Hz, 1H), 8.05-8.03 (d, J = 8.0 Hz, 1H), 7.86-7.82 (t, J = 7.6 Hz , 1H), 4.10-4.08 (d, J = 7.2 Hz, 2H) 1.97 (m, 1H), 1.22 (m, 16H), 0.87-0.80 (m, 6H).

Synthesis of 6-bromo-2-(2-hexyldecyl)-1H-benzo[de]isoquinoline-1,3(2H)-dione (4B)

The synthetic procedure is similar as described for **4A**. Yield: 4.51 g, 60%. ^{1}H NMR (400 MHz, CDCl$_3$, ppm): δ 8.62-8.60 (d, J = 7.2 Hz, 1H), 8.53-8.51 (d, J = 8.4 Hz, 1H), 8.38-8.36 (d, J = 7.6 Hz, 1H), 8.01-8.79 (d, J = 7.6 Hz, 1H), 7.83-7.79 (t, J = 8.0 Hz, 1H), 4.08-4.06 (d, J = 7.2 Hz, 2H), 1.94 (m, 1H), 1.20 (m, 24H), 0.83-0.79 (m, 6H).

Synthesis of 2-(2-butyloctyl)-6-(thiophen-2-yl)-1H-benzo[de]isoquinoline-1,3(2H)-dione (5A)

6-Bromo-2-(2-butyloctyl)-1*H*-benzo[*de*]isoquinoline-1,3(2*H*)-dione (2.67 g, 6.0 mmol), 2-tributylstannylthiophene (2.80 g, 7.5 mmol), [1,1'-bis(diphenylphosphino)ferrocene]dichloropalladium (II) (Pd(dppf)Cl$_2$, 0.22 g, 0.30 mmol) were dissolved in dry toluene (25.0 mL) and then the reaction mixture was heated under reflux overnight under N$_2$ atmosphere. After the reaction mixture was cooled to room temperature, water and EA were added. The aqueous phase was extracted with 100 mL of EA 3 times and combined organic layer was dried over anhydrous Na$_2$SO$_4$. The solvent was removed under the vacuum and the residue was purified by column chromatography (SiO$_2$, hexane: EA, 10:1 (v/v)) afforded a yellow solid (1.81 g, 67.2%). ^{1}H NMR (400 MHz, CDCl$_3$, ppm): δ 8.65-8.59 (m, 3H), 7.83-7.81 (d, J = 7.6 Hz, 1H), 7.78-7.74 (t, J = 8.4 Hz, 1H), 7.55-7.54 (d, J = 4.8 Hz,

1H), 7.35-7.34 (d, *J* = 3.6 Hz, 1H), 7.23 (m, 1H), 4.13-4.11 (d, *J* = 7.2 Hz, 2H) 1.99 (m, 1H), 1.23 (m, 16H), 0.88-0.81 (m, 6H). ^{13}C NMR (<mark>100 MHz</mark>, CDCl₃, ppm): δ 164.57, 164.32, 139.77, 139.00, 132.23, 131.41, 130.70, 129.96, 128.83, 128.64, 127.90, 127.57, 127.18, 122.93, 121.95, 44.52, 36.57, 31.84, 31.67, 31.35, 29.73, 28.70, 26.48, 23.09, 22.64, 14.13, 14.10.

Synthesis of 2-(2-hexyldecyl)-6-(thiophen-2-yl)-1H-benzo[de]isoquinoline-1,3(2H)-dione (5B)

The synthetic procedure is similar to that described for **5A**. Yield: 1.97 g, 65%. ^{1}H NMR (400 MHz, CDCl₃, ppm): δ 8.64-8.58 (m, 3H), 7.82-7.80 (d, *J* = 7.6 Hz, 1H), 7.77-7.73 (t, *J* = 8.4 Hz, 1H), 7.55-7.54 (d, *J* = 6.0 Hz, 1H), 7.34-7.33 (d, *J* = 4.4 Hz, 1H), 7.23 (m, 1H), 4.13-4.11 (d, *J* = 7.2 Hz, 2H) 1.99 (m, 1H), 1.22 (m, 24H), 0.85-0.82 (m, 6H). ^{13}C NMR (<mark>100 MHz, CDCl₃</mark>, ppm): δ 164.55, 164.30, 139.76, 138.98, 132.22, 131.40, 130.69, 129.93, 128.83, 128.79, 128.63, 127.90, 127.57, 127.17, 122.92, 121.93, 44.54, 36.58, 31.88, 31.85, 31.70, 31.66, 30.03, 29.74, 29.56, 29.29, 27.83, 26.89, 26.50, 26.48, 22.66, 14.14.

Synthesis of 6-(5-bromothiophen-2-yl)-2-(2-butyloctyl)-1H-benzo[de]isoquinoline-1,3(2H)-dione (6A)

2-(2-Butyloctyl)-6-(thiophen-2-yl)-1*H*-benzo[*de*]isoquinoline-1,3(2*H*)-dione (1.34 g, 3 mmol) was dissolved in DMF under nitrogen atmosphere, and the *N*-bromosuccinimide (NBS; 0.80 g, 4.5 mmol) was added in one portion. The reaction mixture was stirred overnight at room temperature and then the mixture was quenched with 50 mL of water and extracted with EA. The combined organic extract was with aqueous NaHSO₃ (10 wt.%) and concentrated under reduced pressure to afford a crude product that was purified to column chromatography using hexane:EA (9:1, v/v) to get product as a yellow solid (1.26 g, 80%). ^{1}H NMR (400 MHz, CDCl₃, ppm): δ 8.65-8.63 (d, *J* = 7.2 Hz, 1H), 8.59-8.56 (m, 2H), 7.79-7.75 (t, *J* = 7.2 Hz, 2H), 7.20-7.19 (d, *J* = 4.0 Hz, 1H), 7.09-7.08 (d, *J* = 4.0 Hz, 1H), 4.12-4.11 (d, *J* = 7.2 Hz, 2H) 1.99

(m, 1H), 1.22 (m, 16H), 0.87-0.81 (m, 6H). ^{13}C NMR (100 MHz, CDCl$_3$, ppm): δ 164.43, 164.16, 141.23, 137.76, 131.76, 131.52, 130.73, 130.63, 129.78, 129.08, 128.78, 128.57, 127.41, 123.01, 122.37, 114.4, 44.54, 36.56, 31.84, 31.66, 31.33, 29.73, 28.68, 26.47, 23.08, 22.64, 14.12, 14.10.

Synthesis of 6-(5-bromothiophen-2-yl)-2-(2-hexyldecyl)-1H-benzo[de]isoquinoline-1,3(2H)-dione (6B)

The synthetic procedure is similar to that described for **6A**. Yield: 1.40 g, 80%. ^{1}H NMR (400 MHz, CDCl$_3$, ppm): δ 8.64-8.62 (d, J = 7.2 Hz, 1H), 8.58-8.55 (m, 2H), 7.78-7.74 (t, J = 7.2 Hz, 2H), 7.20-7.19 (d, J = 4.0 Hz, 1H), 7.09-7.08 (d, J = 3.6 Hz, 2H), 4.12-4.10 (d, J = 7.2 Hz, 2H) 1.98 (m, 1H), 1.22 (m, 24H), 0.87-0.81 (m, 6H). ^{13}C NMR (100 MHz, CDCl$_3$, ppm): δ 164.39, 164.12, 141.24, 137.73, 131.71, 131.49, 130.72, 130.60, 129.76, 129.06, 128.77, 128.54, 127.39, 123.06, 122.38, 114.39, 44.57, 36.57, 31.86, 31.83, 31.70, 31.66, 30.01, 29.71, 29.54, 29.27, 26.48, 22.64, 22.63, 14.11, 14.08.

*Synthesis of **NAI-FN-NAI (BO)***

In a round bottom flask 2,7-bis-(4,4,5,5-tetramethyl-[1,3,2]dioxaborolan-2-yl)-fluoren-9-one (100 mg, 0.232 mmol), 6-(5-bromothiophen-2-yl)-2-(2-butyloctyl)-1*H*-benzo[*de*]isoquinoline-1,3(2*H*)-dione (305.4 mg, 0.58 mmol), and 2 M aqueous K$_2$CO$_3$ solution (6 mL) were dissolved in degassed toluene (18 mL). The solution was purged with argon for 30 minutes, then tetrakis(triphenylphosphine)palladium (16.18 mg 0.014 mmol) was added. The reaction was stirred at 110 ºC for 2 days. Then the reaction mixture was cooled to room temperature and extracted with chloroform and water. The organic layer was dried over anhydrous Na$_2$SO$_4$ and concentrated by evaporation. The crude product was purified through column chromatography (SiO$_2$, hexane: chloroform = 1:2). Reddish powder was then washed by hot acetone to afford title compound (169 mg, 68%). ^{1}H NMR (400 MHz, CDCl$_3$, ppm): δ

8.68-8.66 (d, J = 8.8 Hz, 2H), 8.63-8.62 (d, J = 6.4 Hz, 2H), 8.58-8.56 (d, J = 7.6 Hz, 2H), 7.91(s, 2H), 7.83-7.81 (d, J = 7.6 Hz, 2H), 7.78-7.75 (m, 4H), 7.53-7.49 (m, 4H), 7.34-7.33 (d, J = 3.6 Hz, 2H), 4.11-4.09 (d, J = 7.2 Hz, 4H), 1.98 (m, 2H), 1.22 (m, 34H), 0.87-0.80 (m, 12H). ^{13}C NMR (100 MHz, CDCl$_3$, ppm): δ 192.84,164.40, 164.14, 145.09, 143.06, 139.81, 138.26, 135.09, 134.76, 131.91, 131.68, 131.45, 130.67, 130.05, 129.57, 128.85, 128.35, 127.30, 124.53, 123.00, 122.05, 121.40, 121.06, 44.52, 36.57, 31.845, 31.67, 31.34, 29.74, 28.69, 26.48, 23.09, 22.65, 14.13, 14.10, 12.90. Anal. Calcd. for C$_{69}$H$_{70}$N$_2$O$_5$S$_2$: C, 77.35; H, 6.59; N, 2.61. Found: C, 77.04; H, 6.61; N, 2.62.

*Synthesis of **NAI-FN-NAI (HD)***

The synthetic procedure is similar to that described for **NAI-FN-NAI (BO)**. Yield: 187 mg, 65%. ^{1}H NMR (400 MHz, CDCl$_3$, ppm): δ 8.72-8.69 (d, J = 8.4 Hz, 2H), 8.67-8.65 (d, J = 7.2 Hz, 2H), 8.63-8.61 (d, J = 7.6 Hz, 2H), 7.99 (s, 2H), 7.87-7.85 (d, J = 7.6 Hz, 2H), 7.82-7.78 (m, 4H), 7.60-7.58 (d, J = 7.2 Hz, 2H), 7.53-7.52 (d, J = 3.6 Hz, 2H), 7.37-7.36 (d, J = 3.6 Hz, 2H), 4.13-4.12 (d, J = 7.2 Hz, 4H), 2.00 (m, 2H), 1.23 (m, 48H), 0.86-0.82 (m, 12H). ^{13}C NMR (100 MHz, CDCl$_3$, ppm): δ 192.98, 164.47, 164.21, 145.15, 143.18, 139.83, 138.35, 135.86, 135.20, 134.85, 131.98, 131.80, 131.50, 130.72, 129.69, 128.89, 128.42, 127.33, 124.57, 123.04, 122.13, 121.54, 121.13, 44.58, 36.62, 36.59, 31.88, 31.85, 31.71, 31.67, 30.04, 29.74, 29.56, 29.29, 26.48, 22.66, 22.65, 14.13, 14.11. Anal. Calcd. for C$_{77}$H$_{86}$N$_2$O$_5$S$_2$: C, 78.13; H, 7.32; N, 2.37. Found: C, 77.82; H, 7.35; N, 2.39.

*Synthesis of **NAI-FCN-NAI (BO)***

NAI-FN-NAI (BO) (250 mg, 0.233 mol) and malononitrile (31 mg, 0.468 mmol) were dissolved in dried CH$_2$Cl$_2$ (20 mL) under argon, then TiCl$_4$ (0.14 mL, 1.24 mmol) and pyridine were added dropwise at 0 °C. The resulting mixture was stirred overnight at room temperature, and poured into HCl aqueous solution (1M, 40 mL). The mixture was extracted with CH$_2$Cl$_2$

and dried over anhydrous Na_2SO_4. After evaporating the solvent, the crude product was purified through column chromatography (SiO_2, hexane: chloroform = 1:2). And then then recrystallized in acetone to give a green solid (198 mg, 76%). ^1H NMR (400 MHz, $CDCl_3$, ppm): δ 8.72 (s, 2H), 8.67-8.63 (m, 4H), 8.60-8.58 (d, J = 7.6 Hz, 2H), 7.85-7.83(d, J = 7.6 Hz, 2H), 7.81-7.76 (m, 4H), 7.63-7.61 (d, J = 8.0 Hz, 2H), 7.54-7.53 (d, J = 4.0 Hz, 2H), 7.35-7.34 (d, J = 3.6 Hz, 2H), 4.13-4.11 (d, J = 7.2 Hz, 4H), 2.00 (m, 2H), 1.24 (m, 32H), 0.88-0.81 (m, 12H). ^{13}C NMR (100 MHz, $CDCl_3$, ppm): δ 164.18, 163.93, 160.16, 160.12, 144.27, 140.68, 140.30, 137.81, 134.89, 134.81, 131.59, 131.49, 131.32, 130.47, 130.11, 129.26, 128.69, 128.26, 127.30, 124.88, 123.53, 122.92, 122.00, 121.32, 113.03, 44.50, 36.56, 31.84, 31.67, 31.33, 29.75, 28.67, 26.47, 23.09, 22.65, 14.13, 14.10. Anal. Calcd. for $C_{72}H_{70}N_4O_4S_2$: C, 77.25; H, 6.30; N, 5.00. Found: C, 77.56; H, 6.27; N, 4.98.

ASSOCIATED CONTENT

Supporting Information

^{1}H-NMR and ^{13}C-NMR spectra of all synthesized compounds. This material is available free of charge via the Internet at http://pubs.acs.org.

AUTHOR INFORMATION

Corresponding Author

*E-mail: sonar.prashant@qut.edu.au.

Author Contributions

The manuscript was written through contributions of all authors. All authors have given approval to the final version of the manuscript.

ACKNOWLEDGMENT

REFERENCES

(1) Ma, W.; Tumbleston, J. R.; Ye, L.; Wang, C.; Hou, J.; Ade, H. Quantification of Nano- and Mesoscale Phase Separation and Relation to Donor and Acceptor Quantum Efficiency, J(sc), and FF in Polymer:Fullerene Solar Cells. *Adv. Mater.* **2014**, *26*, 4234-4241.

(2) Zhang, F.; Mammo, W.; Andersson, L. M.; Admassie, S.; Andersson, M. R.; Inganäs, O. Low-Bandgap Alternating Fluorene Copolymer/Methanofullerene Heterojunctions in Efficient Near-Infrared Polymer Solar Cells. *Adv. Mater.* **2006**, *18*, 2169-2173.

(3) Liao, S. H.; Jhuo, H. J.; Yeh, P. N.; Cheng, Y. S.; Li, Y. L.; Lee, Y. H.; Sharma, S.; Chen, S. A. Single Junction Inverted Polymer Solar Cell Reaching Power Conversion Efficiency 10.31% by Employing Dual-Doped Zinc Oxide Nano-Film as Cathode Interlayer. *Sci. Rep.* **2014**, *4*, 6813.

(4) Liu, Y.; Zhao, J.; Li, Z.; Mu, C.; Ma, W.; Hu, H.; Jiang, K.; Lin, H.; Ade, H.; Yan, H. Aggregation and Morphology Control Enables Multiple Cases of High-Efficiency Polymer Solar Cells. *Nat. Commun.* **2014**, *5*, 5293.

(5) Vohra, V.; Kawashima, K.; Kakara, T.; Koganezawa, T.; Osaka, I.; Takimiya, K.; Murata, H. Efficient Inverted Polymer Solar Cells Employing Favourable Molecular Orientation. *Nat. Photonics* **2015**, *9*, 403-408.

(6) Yusoff, A. R. b. M.; Kim, D.; Kim, H. P.; Shneider, F. K.; da Silva, W. J.; Jang, J. A High Efficiency Solution Processed Polymer Inverted Triple-Junction Solar Cell Exhibiting a Power Conversion Efficiency of 11.83%. *Energy Environ. Sci.* **2015**, *8*, 303-316.

(7) Sonar, P.; Singh, S. P.; Li, Y.; Ooi, Z. E.; Ha, T. J.; Wong, I.; Soh, M. S.; Dodabalapur, A. High Mobility Organic Thin Film Transistor and Efficient Photovoltaic Devices Using Versatile Donor–Acceptor Polymer Semiconductor by Molecular Design. *Energy Environ. Sci.* **2011**, *4*, 2288-2296.

(8)   Chatterjee, S.; Ie, Y.; Karakawa, M.; Aso, Y. Naphtho[1,2-c:5,6-c']bis[1,2,5]thiadiazole-Containing π-Conjugated Compound: Nonfullerene Electron Acceptor for Organic Photovoltaics. *Adv. Funct. Mater.* **2016**, *26*, 1161-1168.

(9)   Bin, H.; Zhang, Z. G.; Gao, L.; Chen, S.; Zhong, L.; Xue, L.; Yang, C.; Li, Y. Non-Fullerene Polymer Solar Cells Based on Alkylthio and Fluorine Substituted 2D-Conjugated Polymers Reach 9.5% Efficiency. *J. Am. Chem. Soc.* **2016**, *138*, 4657-4664.

(10) Liu, T.; Meng, D.; Cai, Y.; Sun, X.; Li, Y.; Huo, L.; Liu, F.; Wang, Z.; Russell, T. P.; Sun, Y. High-Performance Non-Fullerene Organic Solar Cells Based on a Selenium-Containing Polymer Donor and a Twisted Perylene Bisimide Acceptor. *Adv. Sci.* **2016**, *3*, 1600117.

(11) Lin, Y.; He, Q.; Zhao, F.; Huo, L.; Mai, J.; Lu, X.; Su, C. J.; Li, T.; Wang, J.; Zhu, J.; Sun, Y.; Wang, C.; Zhan, X. A Facile Planar Fused-Ring Electron Acceptor for As-Cast Polymer Solar Cells with 8.71% Efficiency. *J. Am. Chem. Soc.* **2016**, *138*, 2973-2976.

(12) Lin, Y.; Zhao, F.; He, Q.; Huo, L.; Wu, Y.; Parker, T. C.; Ma, W.; Sun, Y.; Wang, C.; Zhu, D.; Heeger, A. J.; Marder, S. R.; Zhan, X. High-Performance Electron Acceptor with Thienyl Side Chains for Organic Photovoltaics. *J. Am. Chem. Soc.* **2016**, *138*, 4955-4961.

(13) Zhao, W.; Qian, D.; Zhang, S.; Li, S.; Inganas, O.; Gao, F.; Hou, J. Free Polymer Solar Cells with Over 11% Efficiency and Excellent Thermal Stability. *Adv. Mater.* **2016**, *28*, 4734-4739.

(14) Zhang, J.; Zhang, X.; Xiao, H.; Li, G.; Liu, Y.; Li, C.; Huang, H.; Chen, X.; Bo, Z. 1,8-Naphthalimide-Based Planar Small Molecular Acceptor for Organic Solar Cells. *ACS Appl. Mater. Interfaces* **2016**, *8*, 5475-5483.

(15) Zhang, J.; Zhang, X.; Li, G.; Xiao, H.; Li, W.; Xie, S.; Li, C.; Bo, Z. A Nonfullerene Acceptor for Wide Band Gap Polymer Based Organic Solar Cells. *Chem. Commun.* **2016**, *52*, 469-472.

(16) Zhang, J.; Xiao, H.; Zhang, X.; Wu, Y.; Li, G.; Li, C.; Chen, X.; Ma, W.; Bo, Z. 1,8-Naphthalimide-Based Nonfullerene Acceptors for Wide Optical Band Gap Polymer Solar Cells with an Ultrathin Active Layer Thickness of 35 nm. *J. Mater. Chem. C* **2016**, *4*, 5656-5663.

(17) Kwon, O. K.; Uddin, M. A.; Park, J. H.; Park, S. K.; Nguyen, T. L.; Woo, H. Y.; Park, S. Y. A High Efficiency Nonfullerene Organic Solar Cell with Optimized Crystalline Organizations. *Adv. Mater.* **2016**, *28*, 910-916.

(18) Hendsbee, A. D.; McAfee, S. M.; Sun, J.-P.; McCormick, T. M.; Hill, I. G.; Welch, G. C. Phthalimide-Based π-Conjugated Small Molecules with Tailored Electronic Energy Levels for Use as Acceptors in Organic Solar Cells. *J. Mater. Chem. C* **2015**, *3*, 8904-8915.

(19) Rutledge, L. R.; McAfee, S. M.; Welch, G. C. Design and Computational Characterization of Non-Fullerene Acceptors for Use in Solution-Processable Solar Cells. *J. Phys. Chem. A* **2014**, *118*, 7939-50791.

(20) Lincker, F.; Delbosc, N.; Bailly, S.; De Bettignies, R.; Billon, M.; Pron, A.; Demadrille, R. Fluorenone-Based Molecules for Bulk-Heterojunction Solar Cells: Synthesis, Characterization, and Photovoltaic Properties. *Adv. Funct. Mater.* **2008**, *18*, 3444-3453.

(21) Porzio, W.; Destri, S.; Pasini, M.; Giovanella, U.; Ragazzi, M.; Scavia, G.; Kotowski, D.; Zotti, G.; Vercelli, B. Synthesis and Characterisation of Fluorenone–Thiophene-Based Donor–Acceptor Oligomers: Role of Moiety Sequence upon Packing and Electronic Properties. *New J. Chem.* **2010**, *34*, 1961-1973.

(22) Sonar, P.; Ha, T. J.; Dodabalapur, A. A Fluorenone Based Low Band Gap Solution Processable Copolymer for Air Stable and High Mobility Organic Field Effect Transistors. *Chem. Commun.* **2013**, *49*, 1588-1590.

(23) Sonar, P.; Ha, T. J.; Dodabalapur, A. Synthesis, Characterization and Organic Field Effect Transistor Performance of a Diketopyrrolopyrrole-Fluorenone Copolymer. *Phys. Chem. Chem. Phys.* **2013**, *15*, 7475-7478.

(24) Linares, M.; Scifo, L.; Demadrille, R.; Brocorens, P.; Beljonne, D.; Lazzaroni, R.; Grevin, B. Two-Dimensional Self-Assemblies of Thiophene-Fluorenone Conjugated Oligomers on Graphite: A Joint STM and Molecular Modeling Study. *J. Phys. Chem. C* **2008**, *112*, 6850.

(25) Cheng, Y. J.; Yang, S. H.; Hsu, C.-S. Synthesis of Conjugated Polymers for Organic Solar Cell Applications. *Chem. Rev.* **2009**, *109*, 5868–5923.

(26) Pei, J.; Wen, S.; Zhou, Y.; Dong, Q.; Liu, Z.; Zhang, J.; Tian, W. A Low Band Gap Donor– Acceptor Copolymer Containing Fluorene and Benzothiadiazole Units: Synthesis and Photovoltaic Properties. *New J. Chem.* **2011**, *35*, 385-393.

(27) Holliday, S.; Ashraf, R. S.; Wadsworth, A.; Baran, D.; Yousaf, S. A.; Nielsen, C. B.; Tan, C. H.; Dimitrov, S. D.; Shang, Z.; Gasparini, N.; Alamoudi, M.; Laquai, F.; Brabec, C. J.; Salleo, A.; Durrant, J. R.; McCulloch, I. High-Efficiency and Air-Stable P3HT-Based Polymer Solar Cells with a New Non-Fullerene Acceptor. *Nat. Commun.* **2016**, *7*, 11585.

(28) Tu, W. H.; Tan, Y. Y.; Rege, O.; Manzhos, S. Computational Design of Small Phenothiazine Dyes for Dye-Sensitized Solar Cells by Functionalizations Affecting The Thiophene Unit. *J. Mol. Model.* **2015**, *21*, 1-13.

(29) Tu, W. H.; Tan, Y. Y.; Manzhos, S. Achieving Improved Solar Absorbance of Small Organic Dyes Featuring Quinoidized Five-Membered Heterocycles. *MRS Proc.* **2014**, *1667*, mrss14-1667-b1607-1603.

(30) Song, H.; Gao, Y.; Li, W.; Tian, H.; Yan, D.; Geng, Y.; Wang, F. Synthesis and Characterization of Diketopyrrolopyrrole-Based Conjugated Molecules Flanked by

Indenothiophene and Benzoindenothiophene Derivatives. *J. Mater. Chem. C* **2015**, *3*, 11135-11143.

(31) Hohenberg, P.; Kohn, W. Inhomogeneous Electron Gas. *Phys. Rev. B* **1964**, *136*, B864-B871.

(32) Kohn, W.; Sham, L. J. Self-Consistent Equations Including Exchange and Correlation Effects. *Phys. Rev.* **1965**, *140*, A1133-A1138.

(33) Becke, A. D. Density-Functional Thermochemistry. III. The Role of Exact Exchange. *J. Chem. Phys.* **1993**, *98*, 5648-5652.

(34) Mennucci, B. Polarizable continuum model. *WIREs Comput .Mol .Sci.* **2012**, *2*, 386-404.

(35) Frisch, M. J.; Trucks, G. W.; Schlegel, H. B.; Scuseria, G. E.; Robb, M. A.; Cheeseman, J. R.; Scalmani, G.; Barone, V.; Mennucci, B.; Petersson, G. A.; Nakatsuji, H.; Caricato, M.; Li, X.; Hratchian, H. P.; Izmaylov, A. F.; Bloino, J.; Zheng, G.; Sonnenberg, J. L.; Hada, M.; Ehara, M.; Toyota, K.; Fukuda, R.; Hasegawa, J.; Ishida, M.; Nakajima, T.; Honda, Y.; Kitao, O.; Nakai, H.; Vreven, T.; Montgomery, J. A.; Peralta, J. E.; Ogliaro, F.; Bearpark, M.; Heyd, J. J.; Brothers, E.; Kudin, K. N.; Staroverov, V. N.; Kobayashi, R.; Normand, J.; Raghavachari, K.; Rendell, A.; Burant, J. C.; Iyengar, S. S.; Tomasi, J.; Cossi, M.; Rega, N.; Millam, J. M.; Klene, M.; Knox, J. E.; Cross, J. B.; Bakken, V.; Adamo, C.; Jaramillo, J.; Gomperts, R.; Stratmann, R. E.; Yazyev, O.; Austin, A. J.; Cammi, R.; Pomelli, C.; Ochterski, J. W.; Martin, R. L.; Morokuma, K.; Zakrzewski, V. G.; Voth, G. A.; Salvador, P.; Dannenberg, J. J.; Dapprich, S.; Daniels, A. D.; Farkas, O.; Foresman, J. B.; Ortiz, J. V.; Cioslowski, J.; Fox, D. J. Gaussian 09. *Gaussian, Inc., Wallingford CT* **2009**.

TOC graph
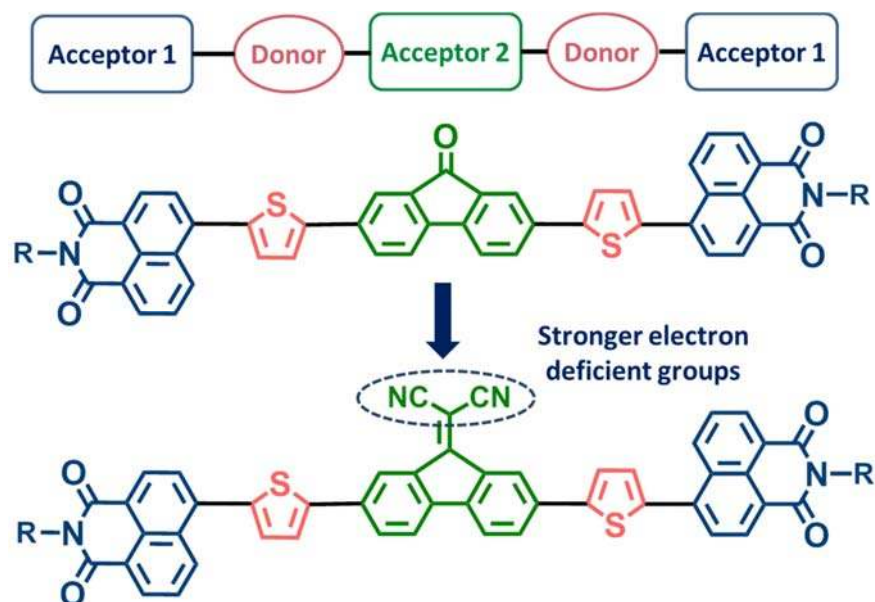
A series of electron deficient small molecules were designed and synthesized with the configuration of acceptor–donor–acceptor–donor–acceptor (A1–D–A2–D–A1), where A1 and A2 where A1 and A2 have different electron affinities.